DOI: 10.1002/chem.200801135

2-Phenanthrenyl–DNA: Synthesis, Pairing, and Fluorescence Properties

Nikolay A. Grigorenko and Christian J. Leumann*[a]

Abstract: Three 2′-phenanthrenyl-*C*-deoxyribonucleosides with donor ($phenNH_2$), acceptor ($phenNO_2$), or no (phenH) substitution on the phenanthrenyl core were synthesized and incorporated into oligodeoxyribonucleotides. Duplexes containing either one or three consecutive phenR residues, which were located opposite each other, were formed. Within these residues, the phenR residues are expected to recognize each other through interstrand stacking interactions, in much the same way as described previously for biphenyl DNA. The thermal, thermodynamic, and fluorescence properties of such duplexes were determined by UV melting analysis and fluorescence spectroscopy. Depending on the nature of the substituent, the thermal stability of single-modified duplexes can vary between −2.7 to +11.3 °C in T_m and that of triple-modified duplexes from +7.8 to +11.1 °C. Van′t Hoff analysis suggested that the observed higher thermodynamic stability in phenH- and $phenNO_2$-containing duplexes is of enthalpic origin. A single phenH or $phenNO_2$ residue in a bulge position also stabilizes a corresponding duplex. If a $phenNO_2$ residue is placed in a bulge position next to a base mismatch this can lead, in a sequence-dependent manner, to duplex destabilization. The $phenNO_2$ residue was found to be a highly efficient (10–100-fold) quencher of phenH and $phenNH_2$ fluorescence if placed in the opposite position to the fluorophores. When phenH and $phenNH_2$ residues were placed opposite each other, efficient quenching of phenH and enhancement of $phenNH_2$ fluorescence was found, which is an indicator for electron- or energy-transfer processes between the aromatic units.

Keywords: DNA recognition · hydrophobic bases · oligonucleotides · phenanthrene · stacking interactions

Introduction

Considerable effort has recently been invested in the design and development of novel DNA base pairs that are orthogonal in their recognition properties when compared with the natural base pairs. Most of these investigations were driven by the search for additional base pairs to be used for the extension of the genetic alphabet,[1–8] as tools in biotechnology,[9–11] for probing recognition, fidelity, and nucleotide processing by DNA polymerases,[12–15] or for designing novel genetic systems.[16,17] Of special interest amongst these artificial constructs are aromatic base replacements that interact with each other, specifically without the formation of hydrogen bonds, merely on the basis of edge-on or face-on hydrophobic or stacking interactions. Interesting examples are shape mimics of the natural base pairs as in the case of, for example, the difluorotoluene/methylbenzimidazole pair,[18] or aromatic units that recognize each other and stabilize duplexes through interstrand stacking interactions as, for example, the propynylcarbostyryl pair.[3,19]

Growing interest for artificial base pairs also comes from the side of materials research and nanosciences. The long-range charge transport through the π stack of the double helix makes DNA an interesting candidate for biosensor applications.[20,21] Moreover, the introduction of metallo base pairs into DNA greatly expands its electronic and magnetic functionality, which is of interest for molecular storage devices and applications as molecular wires and semiconductors.[22–24] The latter field has also recently been reviewed.[25] Thus, there is clear evidence that novel molecular architectures with enhanced functionality based on the DNA double helix can dramatically expand the field of DNA materials.

In a related context, we recently synthesized bipyridyl- and biphenyl–DNA and studied their pairing and spectroscopic properties. We found that multiple consecutive biphenyl pairs can recognize each other through interstrand

[a] Dr. N. A. Grigorenko, Prof. C. J. Leumann
Department of Chemistry & Biochemistry
University of Bern
Freiestrasse 3, 3012 Bern (Switzerland)
Fax: (+41) 31-631-3422
E-mail: leumann@ioc.unibe.ch

Supporting information for this article is available on the WWW under http://dx.doi.org/10.1002/chem.200801135.

stacking interactions in the center of a DNA double helix with a continuing increase in duplex stability.[26–28] A recent NMR structure confirmed the interstrand stacking motif for a system with one biphenyl pair.[29] In addition we could show that the remote biphenyl rings can be equipped with acceptor or donor substituents without alteration of the overall duplex architecture. Such substitutions change the redox potentials of the aromatic systems and lead to remarkable differences in relative affinities, and in some cases to interesting fluorescent properties.[30,31] In a more biological context, biphenyl–DNA has also been investigated by others, for example, as a tool to study the base-flipping mechanism of DNA-alkylating enzymes.[32–34]

However, biphenyl units are not ideally suited for extended stacking interactions owing to the intrinsic non-coplanarity of the phenyl rings. An evident way to overcome this limitation with minimal overall structural changes is by substituting the 4-biphenyl units with 2-phenanthrenyl units. As an additional advantage, phenanthrene shows a slightly larger aromatic surface area compared with biphenyl, which is expected to contribute positively to duplex stability and has more advantageous fluorescence properties. Non-nucleosidic phenanthrene units were previously investigated in the context of DNA architectures as intercalating strand-linking elements[35,36] and have recently been used as stabilizers for triple-helical DNA structures.[37]

Herein we report on the synthesis of three 7-functionalized 2-phenanthrenyl-*C*-nucleosides (Figure 1) their incorporation into oligodeoxyribonucleotides and the investigation of their pairing and fluorescence properties.

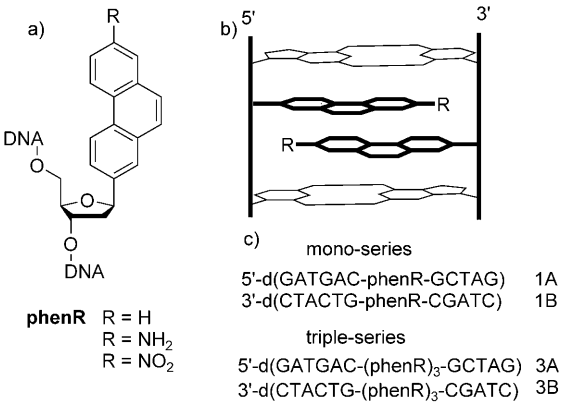

Figure 1. a) Structure of the phenanthrenyl-*C*-nucleoside units; b) cartoon representation of the expected zipper-like duplex structure; c) sequence information of the mono- and triple-modified duplexes. A and B refer to strand A and B, respectively, whereas 1 and 3 designates single or triple modification, respectively. phenR denotes the ensemble of phenH, phenNH_2, or phenNO_2 residues.

Results and Discussion

Synthesis of building blocks: Several methods are known for the selective synthesis of β-configured *C*-nucleosides. These include Heck coupling of glycals with appropriately halogenated aromatic substrates,[38] or addition of metalated aromatic substrates with differently activated glycosyl donors.[39–42] Among the available methods, we have chosen a direct approach that consists of a reaction of the metalated species with TBS-protected 2′-deoxyribolactone followed by reduction of the resulting hemiacetal.[43] Although typically resulting in poorer yields, it is the shortest synthesis and it proceeds stereospecifically. Experimental procedures and analytical characterization of all products and intermediates are contained in the Supporting Information.

2,7-Dibromophenanthrene[44] was monolithiated and reacted with lactone **1**[43] (Scheme 1). Subsequent reduction of the resulting hemiacetal with Et_3SiH in the presence of $BF_3{\cdot}Et_2O$ afforded the mixture of the *C*-nucleosides **2** and **3** in a 16% combined yield and in a 10:1 ratio, both possessing the desired 1′-β-configuration as verified by ^1H NOE experiments. No traces of α-anomers were detected by NMR spectroscopy, thus giving evidence for a greater than 98% selec-

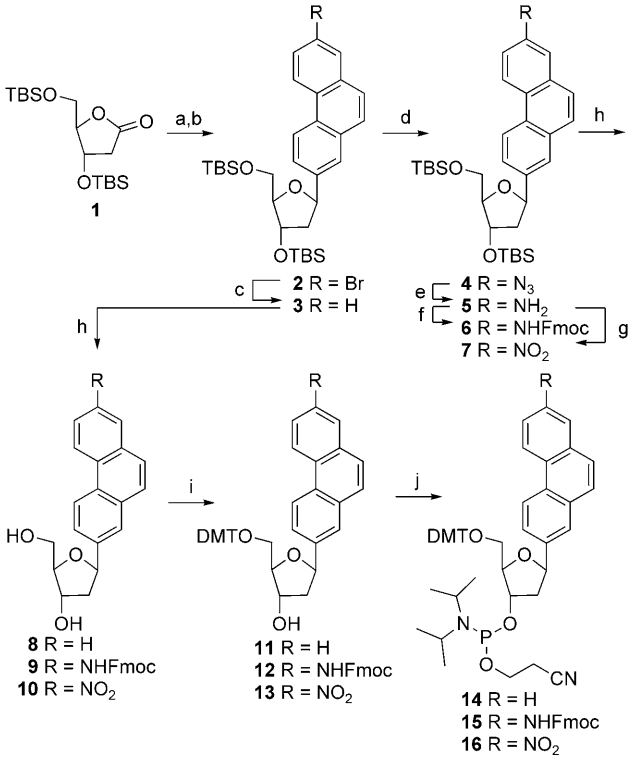

Scheme 1. Reagents and conditions: a) 2,7-dibromophenanthrene, *n*BuLi (1.1 equiv), THF, −78°C, 1 h, then **1** (1 equiv) in THF, −78°C, 4 h; b) Et_3SiH (3 equiv), $BF_3{\cdot}OEt_2$ (3 equiv), CH_2Cl_2, −78°C, 6 h. Yields: **2** (15%), **3** (1.5%); c) *n*BuLi (1.1 equiv), THF, −78°C, 1 h, then H_2O. Yield: quantitative; d) *n*BuLi (1 equiv), THF, −78°C, 40 min, TsN_3 (1.2 equiv), THF, −70°C, 5 h, Na_2HPO_4 (2 equiv), H_2O, Et_2O, THF, +5°C, 12 h. Yield: 91%; e) $SnCl_2$, MeOH, THF, 0°C→RT, 1.5 h. Yield: 85%; f) FmocCl (2 equiv), iPr_2NEt (2 equiv), CH_2Cl_2, RT, 5 h. Yield: 77%; g) dimethyl dioxirane (0.075 M, 4.1 equiv), acetone, MeCN, −80°C, 2 h. Yield: 75%; h) TBAF (1.4 equiv), THF, RT or $(HF)_3{\cdot}NEt_3$ (8 equiv), THF, RT, 24 h. Yield: 75–95%; i) 4,4′-dimethoxytrityl (DMT) chloride (1.2–1.9 equiv), pyridine, 0°C, 5 h. Yield: 73–87%; j) $(iPr_2N)(NCCH_2CH_2O)PCl$ (1.5 equiv), iPr_2NEt (3 equiv), THF, RT, 1.5 h. Yield: 70–83%. Fmoc = 9-fluorenylmethoxycarbonyl, TBAF = tetra-*n*-butylammonium fluoride, TBS = *tert*-butyldimethylsilyl.

tivity in the reduction step. Chromatographic separation of **2** and **3** was unsuccessful at this stage but could be performed after reduction of the azide **4**. Alternatively, the mixture of **2** and **3** could be lithiated and quenched with H_2O to obtain pure **3**.

For the introduction of the functional groups, a convergent approach based on a nitrogen electrophile was chosen. Consequently, bromide **2** was treated with *n*BuLi and reacted with *p*-tosyl azide[45] to give azide **4**, which was subsequently reduced to the amine **5** with $SnCl_2$. The oxidation of amine **5** to the nitro compound **7** was performed with dimethyldioxirane[46] at low temperature (−85 °C) to suppress concomitant hydroxylation as a side reaction and proceeded in 75 % yield. The remaining steps in the synthesis to the phosphoramidites **14–16** were classical functional-group transformations and proceeded as expected.

Design and synthesis of oligonucleotides (ONs): For determination of the recognition properties, two standard sequence contexts were chosen. One sequence (mono-series) contained a single incorporation of a phenR pair and the other (triple-series) contained three contiguous phenR pairs in the center of the duplex (Figure 1). Sequences were designed to contain only one type of phenR-*C*-nucleoside per strand. Owing to the fact that the sequences are not self-complementary, permutational arrangements of donor- and acceptor-substituted phenR residues in the duplex were possible and there was no interference from hairpin formation that had to be taken care of. All ONs were synthesized on a 1.2-μmol scale by using standard protocols for automated DNA synthesis on solid supports except for an extended coupling time (6 min) for the non-natural phosphoramidites. An overview of all synthesized oligonucleotides with mass analytical data is given in Table S1 in the Supporting Information.

Thermal stability of duplexes of the mono series: The thermal stabilities were determined by UV melting curve analysis. A selection of curves is shown in Figure 2. From the T_m data (Table 1), it is clear that there are remarkable differences depending on the nature of the substituents on the phen-core. Insertion of one $phenNO_2$ pair stabilizes the

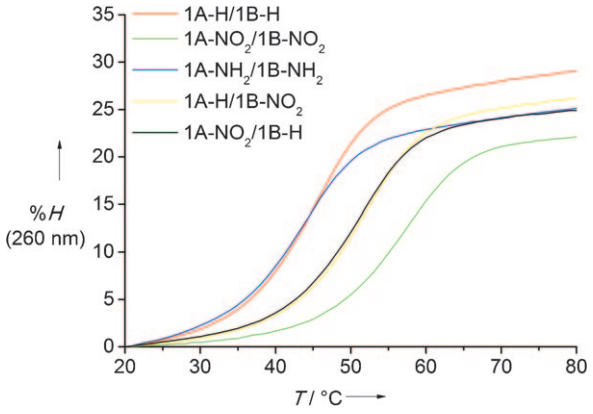

Figure 2. UV melting curves (260 nm) of selected phenR-containing duplexes of the mono series. $c = 1.2$ μM in 10 mM NaH_2PO_4, 0.15 M NaCl, pH 7.0.

Table 1. T_m data (°C) from UV melting curves at 260 nm of duplexes of the mono-series.[a]

	5′-d(GATGAC-phenR-GCTAG) (1A) 3′-d(CTACTG-phenR-CGATC) (1B)				
1A/1B	phenH	$phenNO_2$	$phenNH_2$	dG[b]	del[c]
phenH	45.8	52.4	45.0	47.3	51.0
$phenNO_2$	51.7	57.5	50.8	49.7	53.9
$phenNH_2$	44.8	51.7	43.5	46.3	46.0
dC[b]	41.9	46.7	40.3	51.9	–
del[c]	50.2	53.4	44.2	–	46.2[d]

[a] $c = 1.2$ μM in 10 mM NaH_2PO_4, 0.15 M NaCl, pH 7.0. Estimated error in $T_m = \pm 0.5$ °C. [b] Natural deoxyribonucleotide instead of phenR unit. [c] del = phenR deletion; opposing phenR residue in bulge position. [d] T_m of the phenR-deletion mutant duplex.

duplex by +11.3 °C relative to a deletion mutant duplex, which lacks the phenR pair ($T_m = 46.2$ °C). This is twice the stability as is brought about by one G–C base pair in the same position (+5.7 °C). The unsubstituted phenH pair does not alter the stability significantly and the $phenNH_2$ pair leads to a slight destabilization when compared with the parent deletion mutant duplex. The stability of duplexes with hetero-phenR pairs is in all cases intermediate to the corresponding homo phenR pairs.

Replacement of the phenR units in strand A with natural dC residue (mismatch with natural base) leads to considerable destabilization (up to −10.8 °C in the case of $phenNO_2$) when compared with the duplexes with phenR units in both strands. This is, however, different when the natural base is a purine base. Thus replacement of phenR by G in strand B results in stabilization in the case of phenH and $phenNH_2$, but is still destabilizing for $phenNO_2$. In general, duplexes with phenR residues located opposite to the G residue are more stable than those opposite to the C residue. This is most likely due to the higher hydrophobicity and enhanced stacking interactions of guanine with the opposing phenR unit. When phenR residues were inserted into the bulge positions, $phenNO_2$ is the most stabilizing (+7.7 °C/+7.2 °C), whereas $phenNH_2$ slightly destabilizes the duplex. PhenH shows intermediate stability in relation to $phenNO_2$ and $phenNH_2$.

Thermal stability of the triple-series: The T_m data of duplexes containing three phenR pairs are summarized in Table 2. The consecutive incorporation of three $phenNO_2$ units did not lead to a further increase in T_m, but caused some destabilization as compared to the mono-modified duplex. In fact, the $phenNO_2$ duplex was found to be the least stable among all the triple-modified duplexes. The opposite effect was observed with the phenH and the $phenNH_2$ modifications. In these cases, the additional two nucleotides resulted in a stabilization of 8.7 °C in the case of phenH and 11.6 °C for $phenNH_2$, which is translated into 4.3 °C and 5.8 °C per

Table 2. T_m-data (°C) from UV melting curves at 260 nm of duplexes of the triple series.[a]

	5′-d(GATGAC-(phenR)$_3$-GCTAG) (3A)		
	3′-d(CTACTG-(phenR)$_3$-CGATC) (3B)		
3A/3B	phenH	phenNO$_2$	phenNH$_2$
phenH	54.5	55.4	54.1
phenNO$_2$	56.0	53.3	57.3
phenNH$_2$	54.0	56.8	55.1

[a] $c = 1.2$ μM in 10 mM NaH_2PO_4, 0.15 M NaCl, pH 7.0. Estimated error in $T_m = \pm 0.5$ °C.

Table 3. Thermodynamic data of duplex formation.[a]

	5′-GATGAC-(phenR)$_n$-GCTAG-3′ 3′-CTACTG-(phenR)$_n$-CGATC-5′			
	n	$\Delta G^{298\,K}$ [kcal mol^{-1}]	ΔH [kcal mol^{-1}]	ΔS [cal K^{-1} mol^{-1}]
phenH	1	−13.3	−67.4	−181
phenH	3	−15.2	−69.6	−182
PhenNO$_2$	1	−15.7	−69.3	−180
PhenNO$_2$	3	−14.9	−68.5	−180

[a] Data from $1/T_m$ versus ln(c) plots; concentration range: 0.5–15 μM in 10 mM NaH_2PO_4, 0.15 M NaCl, pH 7.0. Quality of linear fit (R^2) > 0.995.

modification, respectively (Figure 3). Moreover, the stability of the mixed phenNH$_2$/phenNO$_2$ triple-modified duplex was higher than that of both corresponding homo-modified duplexes, suggesting an additional gain in energy owing to electrostatic donor–acceptor interactions.

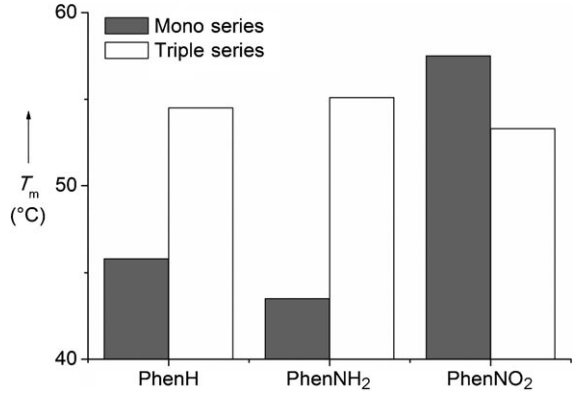

Figure 3. Comparison of T_m data for homo mono- and triple-modified duplexes.

The thermal melting behavior of phenR–DNA follows the same trend as that described earlier for biphenyl–DNA.[30] However, the T_m values for the phenR-containing duplexes are typically higher by 3–7 °C compared with biphenyl-containing duplexes. This is most likely due to the higher stacking surface and the intrinsically flat structure of the phen-core, increasing the hydrophobic effect upon duplex formation and adjusting the geometry of the aromatic unit for easier intercalation.

Thermodynamic data of duplex formation: To obtain more information about the origin of the differences in thermal stability as a function of the phenR units, we measured the thermodynamic parameters of duplex formation by concentration-dependent T_m measurements (van′t Hoff analysis) for the homo phenH and the homo phenNO$_2$ duplexes (mono and triple series). The results are summarized in Table 3.

The free energy changes (ΔG) upon duplex formation are in agreement with the order of thermal duplex stabilities. In all cases, the differences in thermodynamic stability seem to be enthalpy (ΔH) based, whereas the entropy terms are surprisingly constant. Enthalpy-driven complexation of aromatic molecules by various synthetic and natural receptor systems is well established and is described by a nonclassical hydrophobic effect.[47] The data support our model in which the differences between the mono and the triple series, which reflect interactions of the phenR units solely, are mostly due to changes in solvation in the phenH case and to electrostatic or dispersive effects in the phenNO$_2$ case. Both these cases are in line with earlier results on biphenyl–DNA.[30]

Mismatch discrimination: For biotechnological applications, for example, for single nucleotide polymorphism detection, it is desirable to have probes with increased sensitivity for base mismatches. In this context we were interested to determine whether a phenR unit in a bulge position next to a mismatch can modulate its effect on T_m. We thus compared the alteration of duplex stability caused by a single mismatch in presence and absence of a phenR nucleotide in a bulge position on both the 5′- and 3′-side of the mismatch on either strand (Figure 4).

It clearly appears that a phenNH$_2$ bulge in strand A (Figure 4, top) leads to stabilization of all mismatches (4 to 6 °C), except purine–purine mismatches. Incorporation of a phenH in the bulge had an effect analogous to that of PhenNH$_2$, namely considerable stabilization, again with the exception of purine–purine mismatches. Conversely, phenNO$_2$ had little, if any, effect on mismatch T_m. The picture is somewhat different if the bulge is moved to strand B (Figure 4, bottom). In this case, a phenNO$_2$ bulge decreased mismatch T_m values in all cases by 2–5 °C. Only phenNH$_2$ in the bulge had a significant stabilizing effect on A–C and C–C mismatches on the 5′ side of the modification. Generally speaking, phenNO$_2$ in a bulge leads, in most cases, to equal or substantially stronger discrimination of mismatches on either the 3′ or 5′ side of the bulge. As a result, this best fits the profile of a mismatch discrimination enhancer within the three phenR units investigated here. We note, however, that there is considerable sequence dependence. The fact that purine–purine mismatches are more strongly discriminated by a phenR bulge might be due to their preferred structural arrangement in the double helix, which is also intercalative in nature.[48] This prevents the concomitant intercalation of the bulged phenR residue through steric causes.

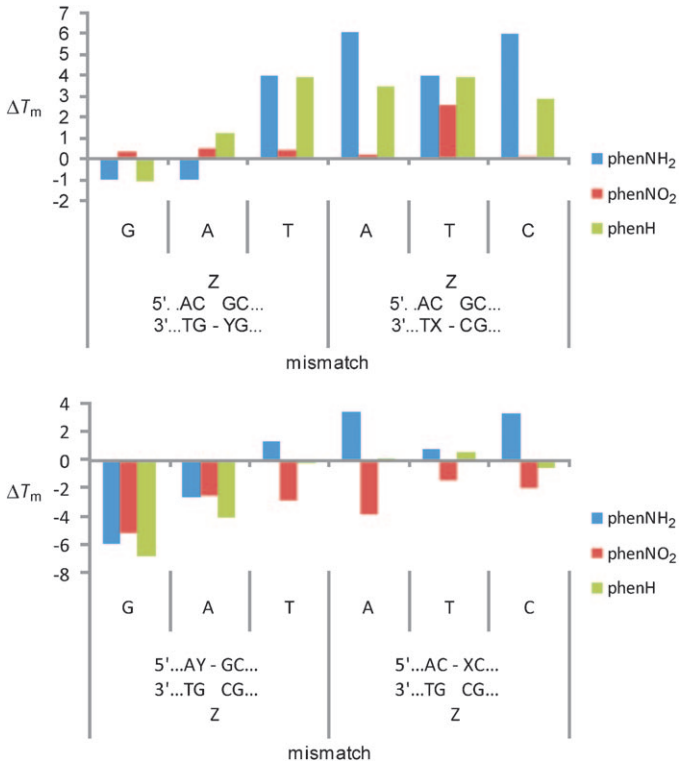

Figure 4. ΔT_m data from UV melting curves (conditions as in Table 2) from mismatched duplexes with and without a phenR residue (Z) in the bulge position next to the mismatch. The phenR-containing strands are from the mono-series strand A (top) and strand B (bottom) that were paired to their mismatched DNA complement.

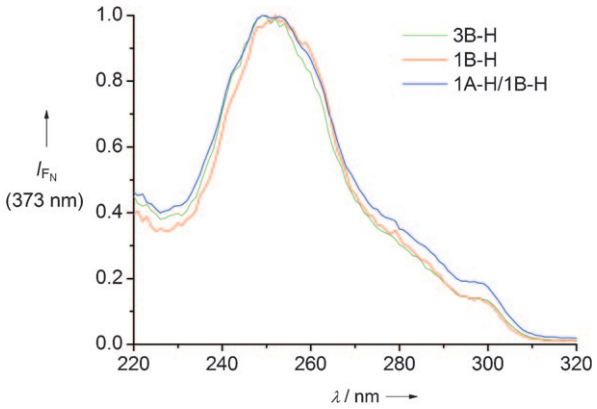

Figure 5. Normalized excitation spectra of ONs 1B-H and 3B-H and duplex 1 A-H/1B-H, monitoring emission intensity at 373 nm ($c = 1.2$ μM ON in 10 mM NaH_2PO_4, 0.15 M NaCl, pH 7.0, $T = 20$ °C). I_f = fluorescence intensity.

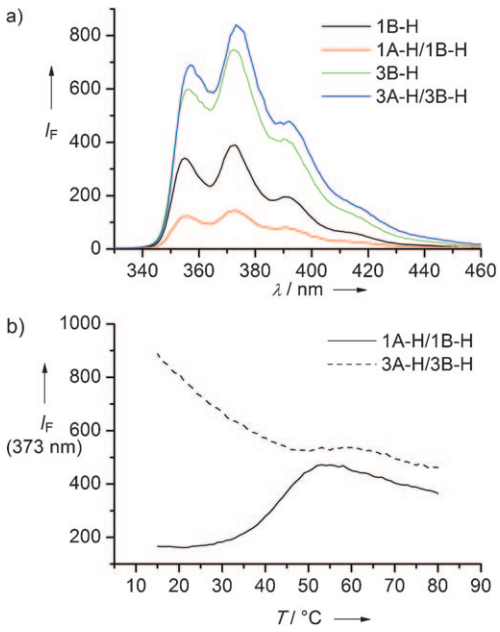

Figure 6. a) Fluorescence spectra of phenH-containing ONs and duplexes. b) Melting curves of the duplexes 1 A-H/1B-H and 3 A-H/3B-H as monitored by the emission intensity at 373 nm. Conditions: excitation wavelength 252 nm; $c = 1.2$ μm duplex in 10 mM NaH_2PO_4, 0.15 M NaCl, pH 7.0; $T = 20$ °C (for a)); heating rate 0.5 °C per min (for b)). I_f = fluorescence intensity.

Fluorescence properties of phenR containing oligonucleotides: We studied the fluorescence properties of phenR-containing ONs both in the single-strand and the duplex state. Single-strand ONs containing one or three phenH insertions show a well-structured emission spectrum with a maximum at 373 nm that, apart from a slight solvent shift, is analogous to the emission spectrum of the corresponding monomeric nucleoside in methanol. The absence of a red-shifted band in the fluorescence spectra of 3B-H and the duplexes 1A-H/1B-H and 3A-H/3B-H indicated no excimer or exciplex formation. Excitation spectra, monitoring emission intensity at 373 nm, revealed a rather broad band with maximum excitation around 250 nm for all phenH ONs (Figure 5). This is in good agreement with the absorption maximum of the parent, free nucleoside (252 nm). The fluorescence intensity of single strands is reduced with increasing temperature in a non-cooperative manner owing to enhanced collisional quenching.

Pairing with a complementary strand leads to a marked quenching of the phenH fluorescence in the case of the mono series (Figure 6a), thus proving the tight positioning of phenH residues inside the base stack relative to neighboring G bases, which are known to quench fluorescence. However, for triple-modified ONs, addition of a complementary strand slightly increases fluorescence intensity. This leads to different fluorescence melting profiles for mono- and triple-modified duplexes, as illustrated in Figure 6b. The vibrational structure in the fluorescence spectrum of the duplexes was nearly completely preserved. Also, in the triple-modified duplex, no red-shifted emission bands were observed below the melting temperature, thus again excluding excimer formation.

The absence of excimer formation is no surprise as phenanthrene itself does not form an excimer under classical conditions.[49] Excimers with emission maxima in the range of 384–432 nm could only be identified when fixed in close proximity in a face-to-face orientation by means of rigid

scaffolds, such as phen-cyclophanes, and also depending on surface overlap and interplanar distance.[50]

Nitroaromatic compounds are generally known to be non-fluorescent, even if the parent hydrocarbon is highly emissive. This is also the case for $PhenNO_2$ units incorporated into ONs that showed no emission upon excitation at 277 nm (maximum of $PhenNO_2$ absorption). Moreover, when paired to complementary ONs with PhenH or $PhenNH_2$ units, $PhenNO_2$-containing ONs acted as excellent quenchers, reducing the fluorescence by 1–2 orders of magnitude in the triple-modified series (Figure 7) and to a slightly reduced extent also in the mono-modified series. This observation calls for tight packing of the phenR-pairs inside the base stack.

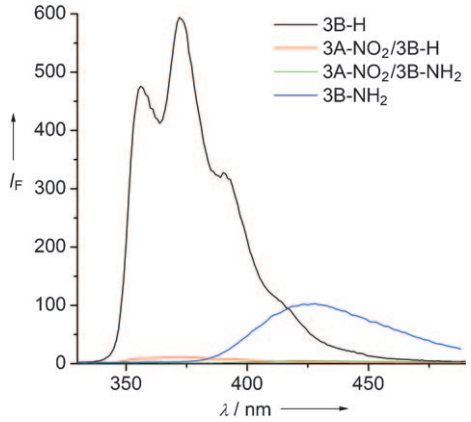

Figure 7. Quenching of phenH and and $phenNH_2$ fluorescence in the triple series upon pairing with a complementary ON containing three $PhenNO_2$ residues. Excitation wavelength: 252 nm (for phen-H) or 264 nm (for $phenNH_2$), $c = 1.2$ μm duplex in 10 mM NaH_2PO_4, 0.15 M NaCl, pH 7.0, $T = 20$ °C. I_f = fluorescence intensity.

Duplexes with mixed phenH/$phenNH_2$ pairs feature interesting fluorescence properties compared with the duplexes with the respective homo-pairs. (Figure 8a). In the mixed arrangement, the phenH emission at 373 nm is completely quenched and the emission at the $phenNH_2$ band is substantially enhanced when excited at the maximum absorbance of the phenH residues at 252 nm. The excitation spectra of the mixed duplex with monitoring of the emission intensity at 425 nm revealed a maximum at 249–250 nm, which corresponds to the maximum absorption of the phenH fragments and not to the maximum absorption of the $phenNH_2$ units (262 nm) (Figure 8b). This observation strongly suggests that emission enhancement at 425 nm is due to electronic coupling of the two chromophores. A similar effect was also observed in the mono-modified series (see the Supporting Information).

Quenching of the excited states of aromatic hydrocarbons by aromatic amines is a well established process and is typically known to proceed through electron transfer.[51] Furthermore, it has been shown that phenanthrene efficiently forms exciplexes with aromatic amines, in particular with *N,N*-dimethylaniline.[52] Given that exciplex emission normally occurs at wavelengths higher than that of the emission of the isolated constituents, we assume again that no exciplex is formed in the 3phenH/3$phenNH_2$ duplex, although we cannot completely rule it out. The mechanistically most-plausible explanation for the observed fluorescence behavior therefore involves charge transfer. Given that stacking of the aromatic moieties in a face-to-face manner is a requirement for efficient charge or energy transfer, our results suggest efficient interstrand interaction of the phenR residues in these duplexes.

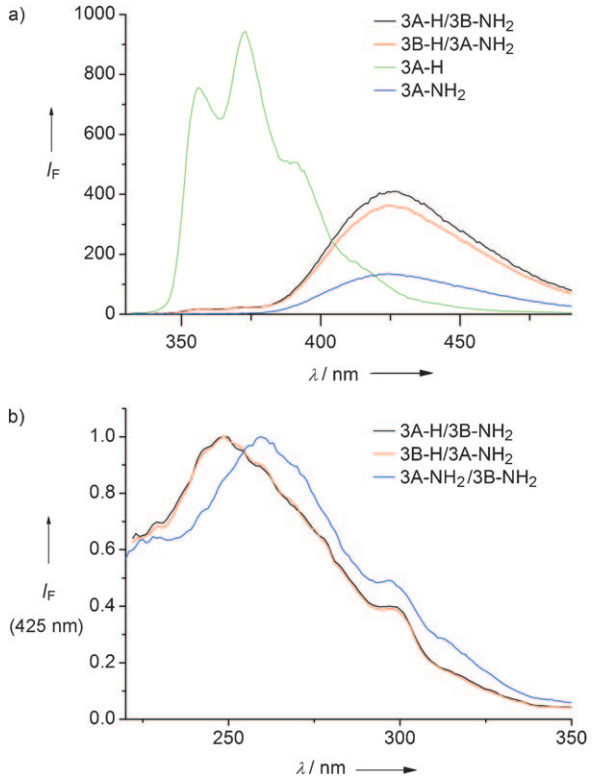

Figure 8. a) Fluorescence emission spectra of the triple-modified duplexses with homo and hetero phenH and $phenNH_2$ pairs and the corresponding single strands. Excitation wavelength: 252 nm; b) normalized excitation spectra monitoring emission at 425 nm. Conditions: $T = 20$ °C, $c =$ 1.2 μm duplex in 10 mM NaH_2PO_4, 0.15 M NaCl, pH 7.0. I_f = fluorescence intensity.

Conclusion

We have prepared a set of novel phenanthrene-*C*-nucleosides that contain donor and acceptor substituents and have incorporated them into oligonucleotides. As observed previously for biphenyl–DNA,[30] these residues, when located in opposite positions in the duplex, most likely organize in a zipper-like interstrand intercalation motif. We observed remarkable differences in thermal stability as a function of the chemical properties of the substituted phenR residues and their interaction with the nearest natural base pairs, or phenR neighbors. The fluorescent properties of these phenR residues in oligonucleotide duplexes range from highly

quenching for the phenNO_2 to emissive for the phenH and phenNH_2 residues. Although no excimer or exciplex formation could be found, a clear electronic coupling between phenH and phenNH_2 residues on opposing strands could be observed most likely by way of charge transfer.

Given the molecular communication between the phenR units, which call for tight face-to-face packing of these residues, and the ease with which the electronic properties of the phen chromophores can be modified by peripheral substitution, it is now of interest to study their electron- or hole-conducting properties in this novel, intercalative DNA recognition motif. First results in this direction were recently disclosed.[53] Novel DNA-based materials with interesting electronic properties are of great current interest in the area of DNA nanomaterials.

Experimental Section

See the Supporting Information for details.

Acknowledgement

Financial support from the Swiss National Science Foundation (grant-No.: 200020—115913) is gratefully acknowledged.

[1] Z. Yang, D. Hutter, P. Sheng, A. M. Sismour, S. A. Benner, *Nucleic Acids Res.* **2006**, *34*, 6095–6101.
[2] Z. Yang, A. M. Sismour, P. Sheng, N. L. Puskar, S. A. Benner, *Nucleic Acids Res.* **2007**, *35*, 4238–4249.
[3] S. Matsuda, J. D. Fillo, A. A. Henry, P. Rai, S. J. Wilkens, T. J. Dwyer, B. H. Geierstanger, D. E. Wemmer, P. G. Schultz, G. Spraggon, F. E. Romesberg, *J. Am. Chem. Soc.* **2007**, *129*, 10466–10473.
[4] A. M. Leconte, S. Matsuda, G. T. Hwang, F. E. Romesberg, *Angew. Chem.* **2006**, *118*, 4432–4435; *Angew. Chem. Int. Ed.* **2006**, *45*, 4326–4329.
[5] I. Hirao, Y. Harada, M. Kimoto, T. Mitsui, T. Fujiwara, S. Yokoyama, *J. Am. Chem. Soc.* **2004**, *126* 13298–13305.
[6] I. Hirao, M. Kimoto, T. Mitsui, T. Fujiwara, R. Kawai, A. Sato, Y. Harada, S. Yokoyama, *Nat. Methods* **2006**, *3*, 729–735.
[7] A. M. Leconte, L. Chen, F. E. Romesberg, *J. Am. Chem. Soc.* **2005**, *127*, 12470–12471.
[8] E. L. Tae, Y. Wu, G. Xia, P. G. Schultz, F. E. Romesberg, *J. Am. Chem. Soc.* **2001**, *123*, 7439–7440.
[9] R. Kawai, M. Kimoto, S. Ikeda, T. Mitsui, M. Endo, S. Yokoyama, I. Hirao, *J. Am. Chem. Soc.* **2005**, *127*, 17286–17295.
[10] M. Kimoto, T. Mitsui, Y. Harada, A. Sato, S. Yokoyama, I. Hirao, *Nucleic Acids Res.* **2007**, *35*, 5360–5369.
[11] M. Berger, Y. Wu, A. K. Ogawa, D. L. McMinn, P. G. Schultz, F. E. Romesberg, *Nucleic Acids Res.* **2000**, *28*, 2911–2914.
[12] T. W. Kim, L. G. Brieba, T. Ellenberger, E. T. Kool, *J. Biol. Chem.* **2006**, *281*, 2289–2295.
[13] J. C. Delaney, P. T. Henderson, S. A. Helquist, J. C. Morales, J. M. Essigmann, E. T. Kool, *Proc. Natl. Acad. Sci. USA* **2003**, *100*, 4469–4473.
[14] L. Dzantiev, O. Alekseyev, J. C. Morales, E. T. Kool, L. J. Romano, *Biochemistry* **2001**, *40*, 3215–3221.
[15] J. C. Morales, E. T. Kool, *Nat. Struct. Biol.* **1998**, *5*, 950–954.
[16] A. T. Krueger, H. Lu, A. H. F. Lee, E. T. Kool, *Acc. Chem. Res.* **2007**, *40*, 141–150.
[17] S. R. Lynch, H. Liu, J. Gao, E. T. Kool, *J. Am. Chem. Soc.* **2006**, *128*, 14704–14711.
[18] K. M. Guckian, T. R. Krugh, E. T. Kool, *J. Am. Chem. Soc.* **2000**, *122*, 6841–6847.
[19] M. Berger, A. K. Ogawa, D. L. McMinn, Y. Q. Wu, P. G. Schultz, F. E. Romesberg, *Angew. Chem.* **2000**, *112*, 3069–3071; *Angew. Chem. Int. Ed.* **2000**, *39* 2940–2942.
[20] T. G. Drummond, M. G. Hill, J. K. Barton, *Nat. Biotechnol.* **2003**, *21*, 1192–1199.
[21] B. M. Zeglis, J. K. Barton, *Nat. Protocols* **2007**, *2*, 357–371.
[22] K. Tanaka, A. Tengeiji, T. Kato, N. Toyama, M. Shionoya, *Science* **2003**, *299*, 1212–1213.
[23] G. H. Clever, K. Polborn, T. Carell, *Angew. Chem.* **2005**, *117*, 7370–7374; *Angew. Chem. Int. Ed.* **2005**, *44*, 7204–7208.
[24] E. Meggers, P. L. Holland, W. B. Tolman, F. E. Romesberg, P. G. Schultz, *J. Am. Chem. Soc.* **2000**, *122*, 10714–10715.
[25] G. H. Clever, C. Kaul, T. Carell, *Angew. Chem.* **2007**, *119*, 6340–6350; *Angew. Chem. Int. Ed.* **2007**, *46*, 6226–6236.
[26] C. Brotschi, A. Häberli, C. J. Leumann, *Angew. Chem.* **2001**, *113*, 3101–3103; *Angew. Chem. Int. Ed.* **2001**, *40*, 3012–3014.
[27] C. Brotschi, C. J. Leumann, *Angew. Chem.* **2003**, *115*, 1694–1697; *Angew. Chem. Int. Ed.* **2003**, *42*, 1655–1658.
[28] C. Brotschi, G. Mathis, C. J. Leumann, *Chem. Eur. J.* **2005**, *11*, 1911–1923.
[29] Z. Johar, A. Zahn, C. J. Leumann, B. Jaun, *Chem. Eur. J.* **2008**, *14*, 1080–1086.
[30] A. Zahn, C. J. Leumann, *Chem. Eur. J.* **2008**, *14*, 1087–1094.
[31] M. Stoop, A. Zahn, C. J. Leumann, *Tetrahedron* **2007**, *63*, 3440–3449.
[32] C. Beuck, I. Singh, A. Bhattacharya, W. Hecker, V. S. Parmar, O. Seitz, E. Weinhold, *Angew. Chem.* **2003**, *115*, 4088–4091; *Angew. Chem. Int. Ed.* **2003**, *42*, 3958–3960.
[33] I. Singh, C. Beuck, A. Bhattacharya, W. Hecker, V. S. Parmar, E. Weinhold, O. Seitz, *Pure Appl. Chem.* **2004**, *76*, 1563–1570.
[34] I. Singh, W. Hecker, A. K. Prasad, V. S. Parmar, O. Seitz, *Chem. Commun.* **2002**, 500–501.
[35] S. M. Langenegger, R. Häner, *Helv. Chim. Acta* **2002**, *85*, 3414–3421.
[36] S. M. Langenegger, R. Häner, *ChemBioChem* **2005**, *6*, 2149–2152.
[37] I. Trkulja, R. Häner, *J. Am. Chem. Soc.* **2007**, *129*, 7982–7989.
[38] K. W. Wellington, S. A. Benner, *Nucleosides Nucleotides Nucleic Acids* **2006**, *25*, 1309–1333.
[39] N. C. Chaudhuri, E. T. Kool, *Tetrahedron Lett.* **1995**, *36*, 1795–1798.
[40] S. Hainke, S. Arndt, O. Seitz, *Org. Biomol. Chem.* **2005**, *3*, 4233–4238.
[41] I. Singh, O. Seitz, *Org. Lett.* **2006**, *8*, 4319–4322.
[42] S. Hainke, I. Singh, J. Hemmings, O. Seitz, *J. Org. Chem.* **2007**, *72*, 8811–8819.
[43] U. Wichai, S. A. Woski, *Bioorg. Med. Chem. Lett.* **1998**, *8*, 3465–3468.
[44] J. W. Ciszek, J. M. Tour, *Tetrahedron Lett.* **2004**, *45*, 2801–2803.
[45] P. Spagnolo, P. Zanirato, S. Gronowitz, *J. Org. Chem.* **1982**, *47*, 3177–3180.
[46] R. W. Murray, S. N. Rajadhyaksha, L. Mohan, *J. Org. Chem.* **1989**, *54*, 5783–5788.
[47] E. A. Meyer, R. K. Castellano, F. Diederich, *Angew. Chem.* **2003**, *115*, 1244–1287; *Angew. Chem. Int. Ed.* **2003**, *42*, 1210–1250.
[48] S.-H. Chou, K.-H. Chin, *J. Mol. Biol.* **2001**, *312*, 753–768.
[49] E. A. Chandross, H. T. Thomas, *J. Am. Chem. Soc.* **1972**, *94*, 2421–2424.
[50] J. Nishimura, Y. Nakamura, Y. Hayashida, T. Kudo, *Acc. Chem. Res.* **2000**, *33*, 679–686.
[51] G. J. Kavarnos, N. J. Turro, *Chem. Rev.* **1986**, *86*, 401–449.
[52] H. Cao, Y. Fujiwara, T. Haino, Y. Fukazawa, C. H. Tung, Y. Tanimoto, *Bull. Chem. Soc. Jap.* **1996**, *69*, 2801–2813.
[53] N. A. Grigorenko, C. J. Leumann, *Chem. Commun.* 2008, 5417–5419.

Received: June 10, 2008
Revised: August 27, 2008
Published online: December 3, 2008

